

MINISTRY OF EDUCATION AND TRAINING  
QUY NHON UNIVERSITY

DUONG VAN LONG

**A QUANTUM CHEMICAL RESEACH OF  
STRUCTURE AND AROMATICITY OF SOME  
BORON CLUSTERS**

Major: Theoretical and Physical Chemistry  
Code No: 9440119

**BRIEF OF DOCTORAL DISSERTATION IN CHEMISTRY**

**BINH DINH – 2023**

The study was completed at Quy Nhon University

Supervisors:

Assoc. Prof. Dr. Nguyen Phi Hung

Prof. Dr. Nguyen Minh Tho

Reviewer 1: Prof. Dr. Nguyen Ngoc Ha

Reviewer 2: Prof. Dr. Tran Thai Hoa

Reviewer 3: Prof. Dr. Duong Tuan Quang

This thesis would be defended for the university level through the evaluation of the Committee at Quy Nhon University at 2:00 PM on December 9, 2023.

The thesis can be found at:

- National library of Vietnam
- The library of Quy Nhon University

# GENERAL INTRODUCTION

## A. Research introduction

The concept of aromaticity emerged as a crucial topic in cluster science for rationalizing thermodynamic stability. However, aromaticity lacks a precise definition due to various qualitative and quantitative models that either support or contradict each other. The well-known Hückel model, originally devised for planar hydrocarbons, is frequently used with its qualitative  $(4n + 2)$  electron counting rule, even for non-planar and three-dimensional structures, neglecting the requirement to solve the secular equation for each structure. This abuse has led to misinterpretations and forgotten the essence of the rule.

In this dissertation, the author aims to establish appropriate models for aromaticity based on rigorous mathematical treatments using different geometrical forms like the circular disk model, the ribbon model, and the hollow cylinder model. These models emphasize the differences and similarities in electron counting rules when dealing with species with geometries significantly distinct from planar organic hydrocarbons.

## B. Objectives and scope of the research

Research objectives: Determination of geometrical structures, electronic configurations and thermodynamic stability of the boron and doped boron clusters. Depending on the different geometries of the obtained clusters, corresponding aromaticity models are used to explain their stability.

Research scopes: The boron and doped boron clusters surveyed in the dissertation include  $B_2Si_3^q$  and  $B_3Si_2^p$  in different charged states,  $B_{70}^{0/2-}$ ,  $B_{12}Li_n$  with  $n = 0 - 14$  and the  $B_{14}FeLi_2$ . The ribbon model joins the Hückel model to explain properties related to  $B_2Si_3^q$  and  $B_3Si_2^p$  clusters. The stability of the quasi-planar isomer of  $B_{70}^{0/2-}$  and the cone-like  $B_{12}Li_4$  is well understood through the disk model. The hollow cylinder model contribute to the elucidation of the properties of  $B_{14}FeLi_2$ .

### C. Novelty and scientific significance

This dissertation aims to clarify the need to distinguish the classical Hückel model from the ribbon model and extended the basic concepts of the ribbon model. The suitability of the TPSSh functional for optimizing structures containing both B and Si is verified through benchmark calculations. The B3LYP functional provides values closer to experimental data for simulating photoelectron spectroscopy or resonant infrared-ultraviolet two-color ionization spectroscopy.

A triplet ground state for a quasi-planar  $B_{70}$  cluster is discovered and confirmed using the topological leapfrog principle. This isomer is predicted to exhibit high thermodynamic stability in the dianion state. The disk model is applied to understand the structure and stability of both neutral and dianionic states, introducing a new electron count for circular disk species.

A comprehensive study of  $B_{12}Li_n$  with  $n = 1-14$  is conducted to understand the growth mechanism of Li doping in boron clusters for potential applications in hydrogen storage materials or Li-ion batteries.  $B_{12}Li_8$  emerges as the most promising candidate for future

experimental investigations as a hydrogen storage material. Additionally, a stable cone-shaped cluster,  $B_{12}Li_4$ , similar to  $B_{13}Li$ , leads to the proposal of a disk-cone model.

The dissertation clarifies the need to distinguish the hollow cylinder model (HCM) from the Hückel model, enabling the rationalization of thermodynamic stability for tubular clusters and predictions for new stable clusters. The stability of  $B_{14}FeLi_2$  is also elucidated using the HCM.

Throughout the dissertation, an original approach and novel findings are achieved, focusing on formulating electron count rules to determine the aromatic character of atomic clusters. These rules are established through rigorous solutions of wave equations tailored to their respective geometric structures.

## **Chapter 1. DISSERTATION OVERVIEW**

### **1.1. Overview of the research**

Cluster science, a field studying atomic clusters consisting of a few to several hundred atoms, has made significant progress alongside materials science advancements. These clusters have diverse applications, including studying catalytic processes, using tiny clusters like  $C_{60}$  for photovoltaic applications, and employing gold clusters in chemical detection through surface-enhanced Raman spectroscopy. Iron oxide clusters are utilized as contrast agents in magnetic resonance imaging for disease diagnosis.

Boron clusters are particularly intriguing due to their electron-deficient nature, unique structures, and electronic properties. With

fewer valence electrons, they exhibit unconventional bonding patterns and various geometries, offering opportunities to explore novel electronic phenomena. Despite challenges in synthesis and characterization, boron clusters hold promise in catalysis, drug delivery, electronics, and energy storage, driving advancements in materials chemistry and cluster science.

The stability of clusters is closely related to aromaticity, and boron clusters follow the Wade-Mingos rule, the Hückel and Baird rules, ...

The stability of a cluster is influenced not only by its size but also its charge state. Doping boron clusters with other atoms or adding electrons can significantly alter their structure and stability.

This doctoral study focuses on investigating the stability of pure and doped boron clusters and explaining their characteristics based on aromaticity models, some of which were developed by the research team including the author. The Hückel and Baird rules are associated with the research results. With the excitement and challenges surrounding boron clusters, this study contributes to advancing the understanding and potential applications of these clusters in various fields.

## **1.2. Objectives of the research**

Geometrical and electronic structures of the boron and doped boron clusters: the neutral and dianionic  $B_{70}$ , the mixed lithium boron  $B_{12}Li_n$  with  $n = 0 - 14$ , the mixed  $B_2Si_3^q$  and  $B_3Si_2^p$ , and the multiply doped  $B_{14}FeLi_2$  boron cluster.

### **1.3. Research content**

The aromaticity models including the conventional Hückel and Barid rules, along with the newly established disk model, ribbon model and hollow cylinder model are used to understand the chemical properties, parameters related to the aromaticity and thereby the thermodynamic stability of the structures investigated.

### **1.4. Research methodology**

#### **1.4.1. Search for lower-lying isomers**

A stochastic search algorithm generates initial geometries for the cluster. Density functional theory with TPSSh and 6-31G(d) basis set is used for optimization. Structures within a 2 eV energy range are re-optimized with a larger 6-311+G(d) basis set to ensure true minima. Gaussian 16 program is used for computations.

#### **1.4.2. ELF – The electron localization function**

The electron localization function (ELF) is used to analyze chemical bonding in clusters based on Pauli repulsion between electrons. It can be divided into  $ELF_{\sigma}$  and  $ELF_{\pi}$  components to assess the aromaticity of  $\sigma$  and  $\pi$  electrons separately. High bifurcation values indicate aromatic species, while low values indicate antiaromatic systems. Dgrid-5.0 software is used for construction, and Gopenmol or ChimeraX software is used for visualization.

#### **1.4.3. Ring current maps**

The SYSMOIC program with the CTOCD-DZ2 method is used to calculate and visualize magnetically induced current density for molecules, providing insight into aromaticity. The anisotropy of induced current density (ACID) is another approach used to demonstrate the aromaticity or antiaromaticity of clusters.

#### **1.4.4. Bond order and net atomic charge**

The net atomic charge (NAC) and bond order for each cluster are carried out using a density partitioning method - the DDEC6 atomic population analysis.

## **Chapter 2. THEORETICAL BACKGROUNDS AND COMPUTATIONAL METHODS**

### **2.1. Theoretical background of quantum computational chemistry**

#### **2.1.1. Schrödinger equation**

The Schrödinger equation is a fundamental equation of quantum mechanics that describes the status of a quantum system. It provides eigenvalues ( $E$ ) representing energy and eigenvectors ( $\psi$ ) representing wave functions.

#### **2.1.2. The Born–Oppenheimer Approximation**

To simplify solving the Schrödinger equation for systems with multiple electrons, the Born-Oppenheimer approximation separates nuclear and electronic motions. The Hamiltonian operator ( $\hat{H}$ ) is split into kinetic energy and potential energy terms for electrons ( $\hat{H}_e$ ) and nuclei ( $H_n$ ).

#### **2.1.3. *Ab initio* computational method**

*Ab initio* methods directly determine the molecular wave function from quantum mechanics equations. Hartree-Fock (HF), Density Functional Theory (DFT), and other post-Hartree-Fock methods like Configuration Interaction (CI) and Coupled Cluster (CC) are commonly used.



#### **2.1.4. The Hartree-Fock Method**

The HF method is a fundamental approach in quantum chemistry that provides a starting point for more advanced methods. It makes approximations like the Born-Oppenheimer approximation, neglecting relativistic effects, using finite basis sets, and considering only single Slater determinants, neglecting electron correlation.

#### **2.1.5. Density Functional Theory**

DFT describes electronic structures by directly considering electron density. The Kohn-Sham equation solves for single-electron wave functions using an effective potential. Exchange-correlation functionals approximate electron correlation effects.

#### **2.1.6. Benchmarking the functional and basis set in DFT**

To assess accuracy, DFT results are compared with higher-level post-Hartree-Fock methods. Researchers choose suitable functionals and basis sets based on system properties, accuracy, and computational resources.

#### **2.1.7. Post-Hartree-Fock methods**

Advanced computational methods (CI, CC, MBPT) incorporate electron correlation more rigorously than HF. CCSD(T) is a widely used gold standard method known for accurate predictions. Complete basis set (CBS) extrapolation reduces basis set dependence.

For spin-contaminated systems, multireference methods like CASSCF and MRCI are needed. CASSCF can be implemented with non-commercial software, while more complex calculations require commercial software and high computational resources.

## 2.2. Aromaticity models in boron clusters

Aromaticity models are an integral part of cluster science, providing insights into the stability, magnetic responses, and various other properties of molecules.

### 2.2.1. The Hückel and Baird rules

The passage explores aromaticity, focusing on benzene using the Hückel model. This model separates cyclic  $C_nH_n$  annulenes into two ensembles: one for  $\sigma$ -framework and the other for  $\pi$ -system.  $\pi$ -electrons are treated as an independent particle system, with molecular orbitals described using p-atomic orbitals. The Hückel model derives the secular determinant, leading to energy levels and molecular orbitals. Benzene, with 6  $\pi$ -electrons, satisfies  $(4n + 2)$  rule, exhibiting aromaticity. Naphthalene (10  $\pi$ -electrons) also follows this rule. However,  $C_4H_4$  and  $C_8H_8$  (4 and 8  $\pi$ -electrons) are antiaromatic due to  $(4n)$  rule. The passage introduces Baird rule for planar, conjugated molecules in the triplet state:  $4n$   $\pi$ -electrons are aromatic,  $(4n + 2)$  are antiaromatic. This rule categorizes triplet states. The passage summarizes the Hückel and Baird rules application in determining aromaticity using electron counting rules for hydrocarbons.

### 2.2.2. Ribbon aromaticity

The passage discusses the ribbon structure of boron derivatives, focusing on their exceptional stability. The electron configuration of  $\pi^{2(n+1)}\sigma^{2n}$  is a common feature in these stable structures. Various analyses, such as the ELF, AdNDP, and NICS, have been used to study their aromaticity. The researcher group proposed a ribbon aromatic model based on an analysis of silicon-doped boron

structures. The model involves a one-dimensional box where electrons move freely, and their energy levels are quantized. The model has been successfully applied to  $B_{14}H_2^{2-}$  and shown to describe both sets of  $\pi$  and  $\sigma$  electrons well.

The ribbon structure's stability is attributed to the alternant interaction of  $ELF_{\pi}$  and  $ELF_{\sigma d}$  basins, leading to an electron configuration of  $\pi^{2(n+1)}\sigma^{2n}$ . However, when the electron configuration is  $\pi^{2n}\sigma^{2n}$ , the structure becomes unstable and is termed a ribbon antiaromatic species. On the other hand, when the electron configuration is  $\pi^{2n+1}\sigma^{2n-1}$ , it exhibits a certain stability and is referred to as a ribbon triplet aromaticity. The analysis is also applied to the dianion  $B_{12}H_2^{2-}$  in singlet and triplet states, showing the differences in their aromatic character.

Overall, the ribbon aromatic model helps explain the exceptional stability of ribbon structures based on their electron configurations, providing insights into their bonding and aromaticity.

### **2.2.3. Disk aromaticity**

The passage discusses the disk aromaticity model, which considers electrons as free particles moving on a plane with infinite walls. The Schrödinger equation for this model is presented in polar coordinates. The solutions are given by Bessel functions, and the eigenfunctions and energies are determined by two quantum numbers: radial ( $n$ ) and rotational ( $m$ ). The rotational quantum numbers are denoted by Greek letters and correspond to different energy levels. The states with non-zero values for  $m$  are 2-fold degenerate. The lowest eigenstates are labelled as  $1\sigma$ ,  $1\pi$ ,  $1\delta$ ,  $2\sigma$ , etc.

#### 2.2.4. Hollow cylinder model

The passage discusses a hollow cylinder model (HCM) represented by the Schrödinger equation in cylindrical coordinates. The HCM is described by a step potential, and its solutions are expressed as wavefunctions with different quantum numbers. The Bessel equation is used to find the wavefunctions, and the energies of the system are determined by three quantum numbers: rational, rotational, and radial. The wavefunction is given by an explicit formula involving Bessel functions.

## Chapter 3. RESULTS AND DISCUSSION

### 3.1. The Hückel rule and the ribbon model: The cases of $B_2Si_3^q$ and $B_3Si_2^p$ clusters

#### 3.1.1. Motivation for the study

In a study on boron or boron-doped clusters, a discrepancy in Lu and co-workers' report regarding  $B_2Si_3^-$  isomers was discovered. The missed isomer was identified as having a global minimum, while the reported isomer was higher in relative energy by 1.9 kcal/mol.

The most stable isomer of  $B_2Si_3$ , **3.2.a**, was found to have conflicting structural predictions: some DFT functionals suggested a perfect planar structure, while others indicated a quasi-planar one.

Isomer **3.2.a** ( **$B_2Si_3.a$** ) had 2  $\pi$  electrons and 2  $\sigma$  delocalized electrons, indicating double aromaticity by the Hückel ( $4n + 2$ ) rule with  $n = 0$ . Another isomer,  **$B_2Si_3.b$** , with higher symmetry, had the same electron configuration as  **$B_2Si_3.a$** . Replacing a Si atom with a B $^-$  ion led to a similar electron configuration in the  $B_3Si_2^-$  structure. All

three structures could be optimized to either a perfect planar or quasi-planar conformation. Doubts were raised about the true double aromaticity of **B<sub>2</sub>Si<sub>3</sub>.a**, **B<sub>2</sub>Si<sub>3</sub>.b**, and **B<sub>3</sub>Si<sub>2</sub><sup>-</sup>**, and further investigations with various charges were conducted to clarify this uncertainty.

### 3.1.2. The benchmarking tests

The study presents global equilibrium structures and lower-lying isomers of **B<sub>2</sub>Si<sub>3</sub><sup>q</sup>** and **B<sub>3</sub>Si<sub>2</sub><sup>p</sup>** with different charges. Benchmark calculations using various functionals and basis sets were conducted to optimize structures containing boron and silicon. The TPSSh, HSE06, and PBE0 functionals are reliable for geometric optimization, while B3LYP yields better results for reproducing some experimental data. The study highlights the importance of selecting appropriate DFT functionals based on specific purposes and properties of atomic species.

### 3.1.3. Ribbon aromaticity model versus the Hückel electron count

The Figure 3.6 illustrate the formation of dianionic isomers **I.B<sub>2</sub>Si<sub>3</sub><sup>2-</sup>** and **II.B<sub>2</sub>Si<sub>3</sub><sup>2-</sup>** by replacing a **B<sup>-</sup>** unit in the trianion **II.B<sub>3</sub>Si<sub>2</sub><sup>3-</sup>** at different positions with an Si atom. All these isomers possess 4  $\pi$  electrons and 2  $\sigma$  delocalized electrons, making them prone to distortion from their planar conformation due to  $\pi$ -antiaromaticity characteristic.

To further understand the influence of the ribbon model on these structures, various analyses are employed, including bond lengths, bond orders, net atomic charges, and the ELF maps. The ribbon model classification reveals that **II.B<sub>3</sub>Si<sub>2</sub><sup>3-</sup>** is a ribbon aromatic structure, while **I.B<sub>3</sub>Si<sub>2</sub><sup>2-</sup>** becomes a ribbon semi-aromatic structure upon removal of a  $\pi$  electron. Additionally, the anion **I.B<sub>3</sub>Si<sub>2</sub><sup>-</sup>** (**C<sub>2v</sub>**) is

categorized as a ribbon antiaromatic species, and the triplet isomer **II.B<sub>3</sub>Si<sub>2</sub><sup>-</sup>** is designated as a ribbon triplet aromatic cluster. Regarding the B<sub>2</sub>Si<sub>3</sub><sup>2-</sup> isomers, both **I.B<sub>2</sub>Si<sub>3</sub><sup>2-</sup>** and **II.B<sub>2</sub>Si<sub>3</sub><sup>2-</sup>** are considered ribbon aromatic species, yet **I.B<sub>2</sub>Si<sub>3</sub><sup>2-</sup>** is more stable due to its geometry being closer to the ribbon motif.

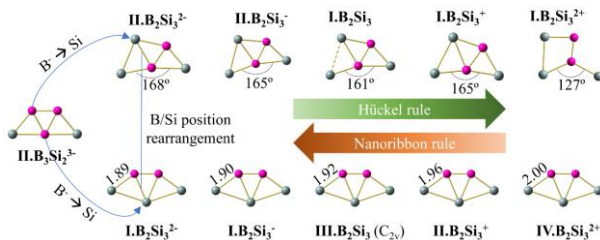


Figure 3.6. A pathway illustrating the evolution leading to the B<sub>2</sub>Si<sub>3</sub><sup>q</sup> from the trianionic ribbon **II.B<sub>3</sub>Si<sub>2</sub><sup>3-</sup>** in which a B<sup>-</sup> unit is replaced by an isovalent Si atom at two different positions leading to two isomeric types, namely ribbon (R) and Hückel (H).

Upon removal of electrons from dianions and anions, the self-lock phenomenon lessens, indicating a gradual change in their aromaticity character. However, the neutral isomers, either <sup>R</sup>**III.B<sub>2</sub>Si<sub>3</sub>** (C<sub>2v</sub>) or <sup>H</sup>**I.B<sub>2</sub>Si<sub>3</sub>**, with 2  $\pi$  and 2  $\sigma$  electrons, can be considered doubly aromatic according to the Hückel electron count, rendering them thermodynamically more stable. In conclusion, the study provides valuable insights into the complexities of ribbon structures and their influence on stability and aromaticity, shedding light on the behavior of these intriguing clusters.

### 3.1.4. Concluding remarks

The study successfully achieved its primary goal of benchmarking the TPSSh/6-311+G(d) method for exploring stable B-Si clusters. However, for reproducing experimental results like

photoelectron spectroscopy or harmonic vibrational frequencies, the B3LYP functional consistently outperformed other methods.

The ribbon aromaticity model categorizes isomers into sub-classes, such as aromaticity, semi-aromaticity, antiaromaticity, and triplet-aromaticity, based on their electronic configurations. Isomers **II.B<sub>3</sub>Si<sub>2</sub><sup>3-</sup>**, **I.B<sub>2</sub>Si<sub>3</sub><sup>2-</sup>**, and **II.B<sub>2</sub>Si<sub>3</sub><sup>2-</sup>** are identified as ribbon aromatic species, while **I.B<sub>3</sub>Si<sub>2</sub><sup>2-</sup>**, **I.B<sub>2</sub>Si<sup>3-</sup>**, and **II.B<sub>2</sub>Si<sub>3</sub><sup>-</sup>** are considered ribbon semi-aromatic species. Ribbon antiaromatic character is assigned to **I.B<sub>3</sub>Si<sub>2</sub><sup>-</sup>** (C<sub>2v</sub>) and **III.B<sub>2</sub>Si<sub>3</sub>** (C<sub>2v</sub>) due to their distortion to lower symmetry (C<sub>2</sub>). The neutral **I.B<sub>2</sub>Si<sub>3</sub>** demonstrates ribbon antiaromaticity but also exhibits more pronounced  $\pi$  aromatic characteristics based on the conventional Hückel rule. The structural changes resulting from adding or removing electrons in both ribbon and Hückel structures lead to corresponding changes in their aromaticity levels.

The competition between the influences of the Hückel model and the ribbon model on the isomers can be summarized in Figure 3.6.

### 3.2. The disk aromaticity on the quasi-planar boron cluster B<sub>70</sub><sup>0/2-</sup>

#### 3.2.1. Motivation of the study

In this study, the topological leapfrog algorithm is applied to investigate the formation of a B<sub>70</sub> quasi-planar (**QP.1**) structure from a B<sub>16</sub> form. The research aims to explain the stability of clusters based on their geometric shapes and establish a general electron counting rule that encompasses both the Hückel and Barid rules.

### 3.2.2. The quasi-planar $B_{70}^{0/2-}$

In this study, the quasi-planar **QP.1** isomer of  $B_{70}$ , derived from the leapfrog algorithm applied to an initial  $B_{16}$  unit, showed a triplet ground state and potential stability as a dianion. Its low ionization energy ( $IE_v = 5.3$  eV) and large two-electron affinity ( $TEA_v \approx 5.6$  eV) suggest thermodynamic stability. The study highlights **QP.1** unique properties and potential experimental detection through anionic and dianionic states using photoelectron spectroscopy (PES).

### 3.2.3. Disk model and electron count rule

The  $\pi$ -electrons of  $B_{70}^{2-}$  follow the spectrum of levels in the disk model (DM). The DM ( $4N + 2M$ ) rule for this dianion, with 50  $\pi$  electrons, satisfies  $N = 11$  and  $M = 3$ . The MO122, MO130, and MO163 correspond to the levels  $1\sigma$ ,  $2\sigma$ , and  $1\sigma$ , respectively (Figure 3.17). The dianion exhibits  $\pi$  disk aromatic character, indicated by diatropic current flows (clockwise arrows) over the outer ring.

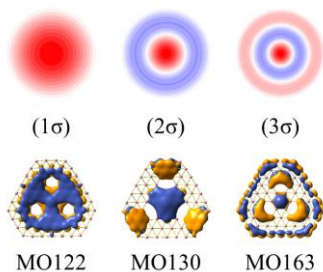


Figure 3.17. Correspondence between the  $\pi$ -MOs of  $B_{70}^{2-}$  with the non-degenerate energy levels of the disk aromaticity model.

Interestingly, the singlet and triplet state of **QP.1** also shows aromaticity, and its electron count follows the  $(4N + 2M)$  and  $(4N + 2M - 2)$  rules, respectively. As the structure becomes smaller, the rules revert back to the Hückel rule of  $(4N + 2)$  and Baird rule of  $(4N)$ , respectively.



### 3.2.4. Concluding remarks

The triplet state of **QP.1** is the most stable isomer among structures close to the planar form of  $B_{70}$ , whereas the dianion state of **QP.1** has high thermodynamic stability and could be eventually identified from photoelectron spectra. The  $(4N + 2M - 2)$  electron count rule is suitable for the neutral triplet ground state, while the  $(4N + 2M)$  rule explains the stability of the  $B_{70}^{2-}$  dianion. The  $(4N + 2M)$  and  $(4N + 2M - 2)$  electron count rules are general electron counting rules for disk-like structures in the singlet and triplet states, respectively. These rules revert to the Hückel and Baird rules when the molecule is small enough in size.

## 3.3. Binary boron lithium clusters $B_{12}Li_n$ with $n = 1-14$ : the disk-cone model for the $B_{12}Li_4$ cluster

### 3.3.1. Motivation of the study

Research on green energy sources, particularly hydrogen energy, is crucial in addressing global warming and sustainable development. Safe hydrogen storage remains an important focus. High hydrogen storage capacity is vital, requiring materials with numerous hydrogen adsorption centers and strong adsorption strength. This study investigates mixed-phase Li-B clusters, particularly  $B_{12}Li_n$  clusters, to identify promising candidates for hydrogen storage materials.  $B_{12}Li_8$  and cone-shaped  $B_{12}Li_4$  structures showed exceptional stability, with emphasis on explaining  $B_{12}Li_4$ 's stability using the disk model in this dissertation.

### 3.3.2. The growth pattern of $B_{12}Li_n$ with $n = 0 - 14$

The study investigates the stability of  $B_{12}Li_n$  clusters with  $n = 0 - 14$ . Many  $B_{12}Li_n$  isomers show similar energy levels.  $B_{12}Li_8$  (**8A**)

exhibits exceptional stability and a unique geometry, making it a promising candidate for hydrogen storage materials. The findings highlight the high thermodynamic stability of  $B_{12}Li_4$ .

### 3.3.3. Relative stabilities of clusters

The study analyzes the relative stabilities of  $B_{12}Li_n$  clusters ( $n = 0 - 14$ ) for the binding energy per atom ( $E_b$ ), dissociation energy ( $\Delta E$ ), and second-order energy difference ( $\Delta_2 E$ ). The  $E_b$  decreases with increasing  $n$  due to weaker B–Li bonds. To explain this, sum of bond orders (SBO) and net atomic charges (NAC) are evaluated, and an average of the sum of bond orders (ASBO) is proposed as a measure of reactivity. The ASBO values correlate with the decrease in  $E_b$ , indicating higher reactivity for clusters with lower ASBO values. The frontier orbital energy gap (HLG),  $\Delta E$ , and  $\Delta_2 E$  diagrams follow a similar trend, with  $B_{12}Li_4$  exhibiting an prominent peak over  $B_{12}Li_2$  and  $B_{12}Li_6$ . Clusters with  $n = 11 - 14$  show saturation and tend towards metallic properties. Some Li atoms in these structures have covalent interactions rather than ionic attractions.

### 3.3.4. Chemical Bonding

The study examines the stability of  $B_{12}Li_n$  clusters ( $n = 0 - 14$ ) for hydrogen storage. Among them, the **14C-T<sub>h</sub>** structure has a perfect electron count but lacks sufficient electron configuration. Distorting **14C-T<sub>h</sub>** leads to the formation of **8A**, a fullerene-like structure with a unique 4-B-atoms bonding motif for Li atoms. The HOMO of **8A** is a strongly bonding orbital, enhancing its thermodynamic stability. The ELF map confirms covalent bonding in **8A**, and it shows potential for capturing molecular hydrogen at Li centers. With a significant energy gap compared to other isomers, **8A** exhibits

promising hydrogen storage capacity, adsorbing up to 40 H<sub>2</sub> molecules (~30% gravimetric density).

### 3.3.5. A mixed cone-disk model

B<sub>12</sub>Li<sub>4</sub> and its conical isomer **4A** are studied in comparison with B<sub>13</sub>Li. **4A** has a cone-shaped structure and is different from the spherical **4C**. It is analyzed using the circular disk model, revealing similar MO shapes to B<sub>13</sub>Li. The HOMO of **4A** resembles the 2σ(π)-orbital of B<sub>13</sub>Li. Both B<sub>13</sub>Li and **4A** exhibit diatropic ring currents, indicating their strong aromaticity.

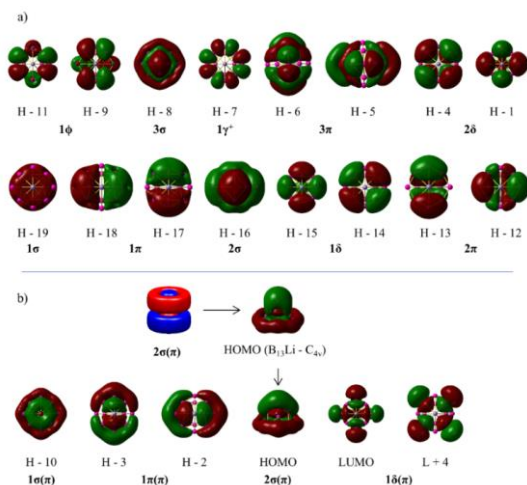


Figure 3.28. Valence MOs and LUMO of the B<sub>13</sub>Li cluster assigned within the circular disk model. H stands for HOMO and L stands for LUMO.

The electronic configurations of these structures are discussed based on the disk and cone models, proposing a mixed cone-disk model (Figure 3.28). The smaller apex angle in cones leads to an earlier appearance of MOs with large radial and small rotational

quantum numbers. The structures are characterized by double aromaticity.

### **3.3.6. Concluding remarks**

The **8A** isomer ( $B_{12}Li_8$ ) exhibits high thermal stability and serves as an excellent candidate for synthesis due to its low energy compared to other isomers. The arrangement of Li atoms around the  $B_{12}$  structure creates an optimal environment for hydrogen adsorption, leading to a remarkable maximum hydrogen storage capacity of up to 30% gravimetric density. The  $B_{12}Li_4$  and  $B_{13}Li$  clusters would propose a mixed cone-disk electron shell model for this type of structures. Additionally, the  $B_{12}Li_4$  size demonstrates superior thermodynamic stability, attributed to the satisfaction of the mixed cone-disk model, making it a doubly aromatic species.

## **3.4. $B_{14}FeLi_2$ and the hollow cylinder model**

### **3.4.1. Motivation of the study**

In 2014, Tam *et al.* reported on a stable  $B_{14}Fe$  cluster in triplet state, with Fe atoms located at the center of the  $B_{14}$  framework. The addition of two Li atoms effectively quenches the magnetic properties of Fe without affecting the stability of the  $B_{14}$  cluster. The hollow cylinder model provides an explanation for the stability of  $B_{14}FeLi_2$ , which is a key aspect of this dissertation.

### 3.4.2. Stability of B<sub>14</sub>FeLi<sub>2</sub> and its potential applications

At the TPSSh/def2-TZVP + ZPE level, the ground state of the B<sub>14</sub>FeLi<sub>2</sub> cluster is a low spin teetotum structure with D<sub>7d</sub> symmetry, composed of two B<sub>7</sub> strings with endohedral-capped Fe and attached Li atoms. The addition of Li atoms affects the inter-ring distance

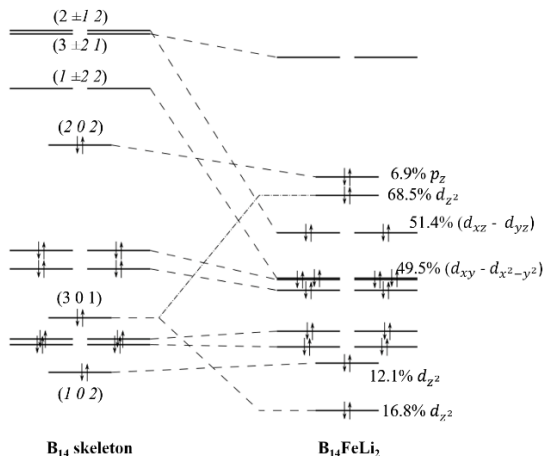


Figure 3.33. Formation of MOs of B<sub>14</sub>FeLi<sub>2</sub> from MOs of singlet B<sub>14</sub> skeleton and a contribution from *d*-AO of Fe atom. Some MOs of the singlet B<sub>14</sub> skeleton are assigned by hollow cylinder model.

only slightly. The teetotum structure has a HOMO-LUMO gap of 2.1 eV, higher than the high spin tubular B<sub>14</sub>Fe. The interaction between the B<sub>14</sub> skeleton and the Li-Fe-Li linear unit leads to the formation of the Li-(Fe@B<sub>14</sub>)-Li teetotum. The (2 0 2)-orbital of the hollow cylinder model contributes to the thermodynamic stability of the structure (Figure 3.33). Insertion of Fe expands B-B bonds, weakening all B-B bonds with peripheral B-B bonds at 1.63 Å and

B-B bonds between rings at 1.79 Å. The ACID analysis has revealed the aromaticity of the  $B_{14}FeLi_2$  cluster. The high symmetry geometry of  $B_{14}FeLi_2$  resulted in forbidden electronic transitions for visible light but absorption of UV light. The study introduced two approaches for creating boron-based nanowires using  $B_{14}FeLi_2$  as the linkage unit, one with Li linkers and another with Mg linkers. Nanowires based on Mg linkers, when extended to infinite units, were extrapolated to have a metallic character with a bandgap of  $\sim 0.8$  eV.

### **3.4.3. Concluding remarks**

The  $B_{14}FeLi_2$  cluster was found to have a teetotum form with a low spin singlet state, making it highly thermodynamically stable. The insertion of Fe atom in  $B_{14}$  expanded peripheral B-B bonds and weakened all B-B bonds. The (2 0 2)-orbital of the hollow cylinder model played a crucial role in shortening the peripheral B-B bonds to 1.63 Å and B-B bonds between two B-strings to  $\sim 1.79$  Å.

The high symmetry geometry of  $B_{14}FeLi_2$  resulted in forbidden electronic transitions for visible light but absorption of UV light. The study introduced two approaches for creating boron-based nanowires using  $B_{14}FeLi_2$  as the linkage unit, one with Li linkers and another with Mg linkers. Nanowires based on Mg linkers, when extended to infinite units, were extrapolated to have a metallic character with a bandgap of  $\sim 0.8$  eV.

## Chapter 4. GENERAL CONCLUSIONS AND FUTURE DIRECTIONS

### 4.1. General Conclusions

In this theoretical study, quantum chemical calculations were performed to determine the geometries, electronic structures, and chemical bonding of several new pure and doped boron clusters with different impurities. During this doctoral study several important results have been achieved. The results obtained for the specific systems were reported in Chapter 3, but for the sake of overview, they are briefly summarized hereafter. More importantly, different aromaticity models were proposed and applied to these systems, depending on the geometry of each structure to account for its thermodynamic stability, and where possible, some of its physicochemical properties involved. The achieved results from these studies include:

i) In terms of methodology, the TPSSh functional is highly reliable for optimizing the geometric structures of clusters containing B atoms, as demonstrated in benchmark tests involving clusters comprising B and either Si or Li. When verification with experimental values related to VDEs or harmonic vibrational frequencies, the B3LYP functional achieves a better agreement for these clusters.

ii) The ribbon model: the study on  $B_2Si_3^q$  with the charge  $q$  going from -2 to 2 and  $B_3Si_2^p$  with the charge  $p$  going from -3 to 1 clarified the difference between the Hückel rule and ribbon model and showed how both models can be used to probe the stability of

these clusters. The ribbon aromaticity model is categorized into subclasses including *aromaticity*, *semi-aromaticity*, *antiaromaticity*, and *triplet-aromaticity* types when the electronic configuration of  $[\dots\pi^{2(n+1)}\sigma^{2n}]$ ,  $[\dots\pi^{2n+1}\sigma^{2n}]$ ,  $[\dots\pi^{2n}\sigma^{2n}]$ , and  $[\dots\pi^{2n+1}\sigma^{2n-1}]$  are involved, respectively. To ensure a structure is classified into a ribbon, a *self-lock* phenomenon needs to be found in that structure. An alternating distribution between  $\pi$  and  $\sigma$  delocalized electrons will subsequently be found in the resulting aromatic ribbon structure.

iii) The disk model: the investigation revisited the stable structure of  $B_{70}$  and discovered that the **QP.1** structure in the triplet state is the most stable quasi-planar form. The existence of the **QP.1** structure is in line with the topological leapfrog principle constrained structures. The QP form of the  $B_{70}^{2-}$  dianion becomes stabilized when two electrons are added to the neutral **QP.1** structure to fill the two open-shell SOMO levels of the neutral state. Ring current maps for **QP.1** in triplet neutral and singlet dianionic states both indicate an aromatic character. The generalized  $(4N + 2M)$  and  $(4N + 2M - 2)$  electron count rules are proposed for the disk model. These models revert to the Hückel or Baird models when the molecule size reduces to a non-degenerate level.

iv) The disk-cone model: a cone-disk electron shell model was proposed through the investigation of the stability of the cone-like  $B_{13}Li$  and  $B_{12}Li_4$  structures. With the electronic configuration  $[1\sigma^21\pi^42\sigma^21\delta^42\pi^41\phi^43\sigma^21\gamma^23\pi^42\delta^4]$  of the  $\sigma$  electron set and  $[1\sigma^21\pi^42\sigma^2]$  of the  $\pi$  electron set, both  $B_{13}Li$  and  $B_{12}Li_4$  are characterized by a double aromaticity. The systematic investigation of lithium doping into  $B_{12}$  revealed that  $B_{12}Li_8$  is a promising cluster to serve as a desirable material for  $H_2$  storage, with a gravimetric



weight ratio of hydrogen is up to 30 wt%, and the interaction energy from the first H<sub>2</sub> to the 40<sup>th</sup> H<sub>2</sub> in the range of 0.15 to 0.08 eV, indicating a behavior being more than a physisorption but less than a chemisorption.

v) The hollow cylinder model: the teetotum B<sub>14</sub>FeLi<sub>2</sub> is a stable structure that does not absorb visible light and is capable of extending into nanowires. When extended, they become conductors when the band gap is extrapolated to about 0.8 eV. Therefore, B<sub>14</sub>FeLi<sub>2</sub> is considered as a material with potential applications in the field of photovoltaics. To account for the stability of this structure, the HCM has been effective in elucidating the formation of their MOs through the hybridization between the MOs of the B<sub>14</sub> framework and the AO of Fe. The HOMO of B<sub>14</sub>FeLi<sub>2</sub> is characterized by the (2 0 2)-orbital of the HCM is also one of the basic reasons which brings in a highly thermodynamically stable structure.

Overall, the intensive work carried out during this doctoral study has led to the proposal of several novel models that account for aromaticity, which remains a fundamental concept in modern chemistry. The new models and electron count rules have been derived through a rigorous mathematical treatment involving the solutions of wave equations adapted for each type of geometry. Up to now, these models have demonstrated successful applications to various types of geometries. Moreover, the classical electron counts that determine the aromatic character have been revealed as the simplest cases within these models.

## **4.2. Future Directions**

The aromatic models, including ribbon, disk, and hollow cylinder models, have gained recognition in prestigious journals and is increasingly gaining popularity within the scientific community in clusters, but these models need to be applied to more clusters in order for their generality to be quickly achieved. Various aromaticity models like spherical aromaticity and the jellium model should be considered for each structure. The goal is to make these models accessible to chemists for better compound and material understanding. The author's future research involves investigating boron and other elemental clusters, understanding their shape, bonding, and the role of aromaticity in thermodynamic stability. The study also explores potential applications like hydrogen adsorption, catalysis, and drug delivery, promising a bright future for atomic clusters.

## LIST OF PUBLICATIONS CONTRIBUTING TO THE DISSERTATION

- 1) Boron Silicon  $B_2Si_3^q$  and  $B_3Si_2^p$  Clusters: The Smallest Aromatic Ribbons. **Long Van Duong**, Nguyen Ngoc Tri, Nguyen Phi Hung, and Minh Tho Nguyen, *J. Phys. Chem. A*, vol. 126, no. 20, pp. 3101–3109, May 2022.
- 2) A topological path to the formation of the quasi-planar  $B_{70}$  boron cluster and its dianion. Pinaki Saha, Fernando Buendia Zamudio, **Long Van Duong**, and Minh Tho Nguyen, *Phys. Chem. Chem. Phys.*, Advance Article, 2023.
- 3) The binary boron lithium clusters  $B_{12}Li_n$  with  $n = 1-14$ : in search for hydrogen storage materials. **Long Van Duong**, Nguyen Thanh Si, Nguyen Phi Hung, and Minh Tho Nguyen, *Phys. Chem. Chem. Phys.*, vol. 23, no. 43, pp. 24866–24877, 2021.
- 4) The teetotum cluster  $Li_2FeB_{14}$  and its possible use for constructing boron nanowires. Ehsan Shakerzadeh, **Long Van Duong**, My Phuong Pham-Ho, Elham Tahmasebi, and Minh Tho Nguyen, *Phys. Chem. Chem. Phys.*, vol. 22, no. 26, pp. 15013–15021, 2020.

### List of conferences

Poster presentation in:

The Asia Pacific Association of Theoretical and Computational Chemistry (APATCC-10) at the International Centre for Interdisciplinary Science and Education (ICISE), Quy Nhon – Vietnam, February 19<sup>th</sup> – 23<sup>rd</sup>, 2023.